Inorganic Chemistry

Article

pubs.acs.org/IC

Dinuclear Zinc Salen Catalysts for the Ring Opening Copolymerization of Epoxides and Carbon Dioxide or Anhydrides

Arnaud Thevenon, Jennifer A. Garden, Andrew J. P. White, and Charlotte K. Williams*

Department of Chemistry, Imperial College London, London, SW7 2AZ, United Kingdom

Supporting Information

ABSTRACT: A series of four dizinc complexes coordinated by salen or salan ligands, derived from *ortho*-vanillin and bearing (±)-*trans*-1,2-diaminocyclohexane ($\mathbf{L_1}$) or 2,2-dimethyl-1,3-propanediamine ($\mathbf{L_2}$) backbones, is reported. The complexes are characterized using a combination of X-ray crystallography, multinuclear NMR, DOSY, and MALDI-TOF spectroscopies, and elemental analysis. The stability of the dinuclear complexes depends on the ligand structure, with the most stable complexes having imine substituents. The complexes are tested as catalysts for the ring-opening copolymerization (ROCOP) of CO_2/cyclohexene oxide (CHO) and phthalic anhydride (PA)/CHO. All complexes are active, and the structure/activity relationships reveal that the complex having both $\mathbf{L_2}$ and imine substituents displays the highest activity. In the ROCOP of CO_2/CHO its activity is equivalent to other metal salen catalysts (TOF = 44 h^{-1} at a catalyst loading of 0.1 mol %, 30 bar of CO_2, and 80 °C), while for the ROCOP of PA/CHO, its activity is slightly higher than other metal salen catalysts (TOF = 198 h^{-1} at a catalyst loading of 1 mol % and 100 °C). Poly(ester-*block*-carbonate) polymers are also afforded using the most active catalyst by the one-pot terpolymerization of PA/CHO/CO_2.

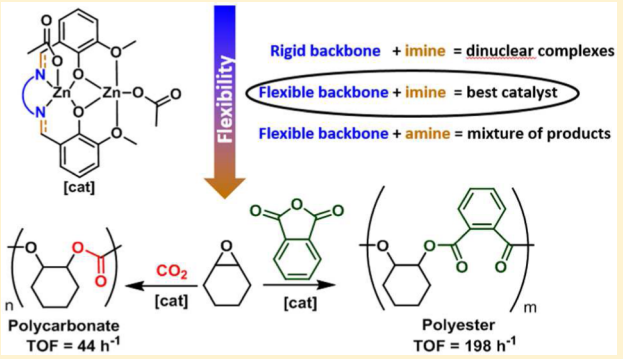

INTRODUCTION

Salen ligands, initially derived from the condensation of salicylaldehyde and ethylenediamine, are of fundamental importance in coordination chemistry and catalysis. They have been extensively studied since the pioneering work of Jacobsen[1] and Katsuki[2] using a chiral [Mn(salen)] complex for the enantioselective epoxidation of alkenes. Since then, a range of other transition metal catalysts have been reported for reactions as distinct as oxidations,[3] polymerizations,[4] and epoxidations.[5] More recently, a novel class of salen ligands have been developed incorporating a Lewis donor functional group in the *ortho* position of the salicylaldehyde unit, enabling the coordination of a second metal center within the ligand scaffold.[6] Dinuclear salen complexes, where two different metals (usually a transition metal and a lanthanide) are incorporated into the ligand, have been studied for their magnetic properties[7] and are even proposed as single-molecule magnets.[8] Such complexes are also attractive catalysts for asymmetric organic reactions, where it is proposed that they show better performances due to cooperative interactions between the two metal centers.[9] Exactly this type of metal cooperation has also been proposed to be an important criterion in the preparation of highly active catalysts for the ring-opening copolymerization (ROCOP) of CO_2 and epoxides.[10]

One of the first well-characterized dinuclear catalysts for CO_2/epoxide ROCOP was a zinc β-diiminate (BDI) complex that was shown to adopt dimeric structures in the most active catalysts.[10d] Since this pivotal finding, many highly active dinuclear catalysts have been developed including those based on macrocyclic,[11] BDI,[10d,12] Trost type "pro-phenolate",[4d,13] porphyrin,[14] and anilido−aldimine[15] ligand scaffolds, typically coordinated to zinc, although other transition metal systems have also been investigated.[16] Mechanistic studies and density functional theory calculations have highlighted that the catalyst activity seems to be highly dependent on the flexibility of the ligand and the distance between the two metal centers.[10a,c,11c,17] To date, one of the most active catalyst systems for the synthesis of poly(cyclohexene carbonate) (PCHC), reported earlier this year by Rieger and co-workers;[18,19] is based on a flexible dizinc complex, coordinated by two β-diiminate moieties that are linked through the phenyl rings (TOF = 155 000 h^{-1} at a catalyst loading of 0.0125 mol %, 100 °C, and 30 bar of CO_2).

Mononuclear salen ligands coordinated to either Co(III) or Cr(III) centers and combined with a Lewis base/ionic cocatalyst have also been widely employed as catalysts for CO_2/epoxide ROCOP.[4i,j,20] In this case, the separation between the metal and the cocatalyst is of key of importance for the high activity.[21] Nozaki and co-workers pioneered a new generation of "cocatalyst tethered" salen complexes, which show a significant improvement in the catalyst activity.[21] The combination of tethering together the salen catalyst and

Received: September 29, 2015

DOI: 10.1021/acs.inorgchem.5b02233
Inorg. Chem. XXXX, XXX, XXX−XXX

cocatalyst was subsequently successfully applied by various researchers,[22] including Lu and Lee, to prepare some of the most active catalysts reported for ROCOP (TOF > 20 000 h^{-1}).[23] A further benefit is that some of these tethered catalysts can be reclaimed from the polymer and recycled without significant loss in performance.[23g]

Another successful strategy, also initially developed by Nozaki and co-workers, has been to join together two distinct metal salen catalysts and to combine them with cocatalysts.[24] Such dinuclear catalysts are coordinated by two salen ancillary ligands that have been covalently linked to one another;[25] the catalysts show higher activity than mononuclear counterparts, particularly at low catalyst loadings.[24,25b] Given the precedence for salen ligands and the promise of dinuclear catalysts, it is perhaps surprising that there is, so far, only a single report of ROCOP catalysts where a single salen ancillary ligand coordinates two metals.[26] The catalyst comprises a multidendate bis(benzotriazole iminophenol) ligand coordinated to two Zn(II), Ni(II), or Co(II) metal centers. The best activities were achieved with the di-Ni(II) catalyst, which for the ROCOP of CHO/CO_2 shows a TOF of 53 h^{-1}, at 120 °C and 20 bar of CO_2.[26] These encouraging results using dinuclear salen catalysts inspired the current development of new dinuclear salen ligands and the investigation of their coordination chemistry and catalytic applications for CO_2/CHO and phthalic anhydride (PA)/CHO ROCOP. When developing new polymerization catalysts, it is attractive to target low-cost ligands, ideally derived from renewables, which can be coordinated to earth-abundant metal centers.[27] *ortho*-Vanillin is an interesting candidate, as it is relatively abundant and straightforward to extract from a range of plants. In addition, *ortho*-vanillin salen ligands have a good precedent for the formation of dinuclear complexes, although these have not yet been applied in this area of polymerization catalysis.[28] Zinc was also selected as the most desirable metal center as it is abundant, nontoxic, and usually results in colorless complexes.

RESULTS AND DISCUSSION

Using *ortho*-vanillin as a starting point, four new ligands were synthesized, isolated, and characterized. As mentioned, *ortho*-vanillin is an attractive starting material, as it is inexpensive and commercially available; furthermore, the targeted ligands were obtained on a large scale in only 1 d, through a simple, one-pot synthetic method (Scheme 1).

Scheme 1. Ligand Syntheses

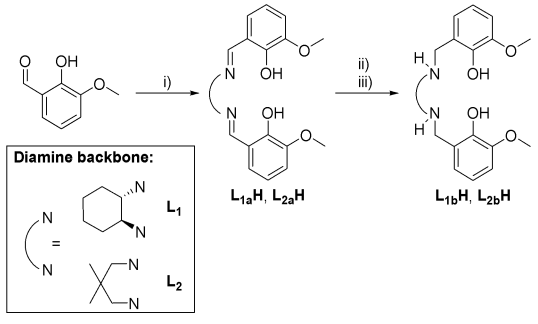

(i) 2 equiv of *o*-vanillin, 1 equiv of corresponding diamine, MeOH, 22 °C, 4 h, (100% yield for $\mathbf{L_{1a}H}$ and $\mathbf{L_{2a}H}$); (ii) 3.5 equiv of $NaBH_4$, MeOH, 22 °C, 2 h; (iii) H_2O, 22 °C, 16 h (97% yield for $\mathbf{L_{1b}H}$ and $\mathbf{L_{2b}H}$).

First, the amination of *ortho*-vanillin, using the relevant diamine [(±)-*trans*-1,2-diaminocyclohexane ($\mathbf{L_1}$) or 2,2-dimethyl-1,3-propanediamine ($\mathbf{L_2}$)], gave the desired imine product ($\mathbf{L_{1a}H}$, $\mathbf{L_{2a}H}$, Scheme 1). The ligands differ according to the diamine "linker" group and were selected on the basis that such C_2 and C_3 linkers are common components of successful ROCOP catalysts.[11a,f,21,23a] Subsequent in situ reduction of the imine moieties on the salen ligands was performed, using $NaBH_4$, to obtain the corresponding amines and salan ligands ($\mathbf{L_{1b}H}$, $\mathbf{L_{2b}H}$, Scheme 1). All four ligands were obtained in near quantitative yields and did not require purification (Figure S1−8).

Metal Complexations. $\mathbf{L_{1a}H}$, $\mathbf{L_{1b}H}$, and $\mathbf{L_{2a}H}$ were reacted with 2 equiv of [$Zn(OAc)_2{\cdot}2(H_2O)$] to afford the corresponding bis(zinc acetate) complexes (Scheme 2) in good yields (62−68%).

Scheme 2. Complexation Reactions of the Ligands with Zinc

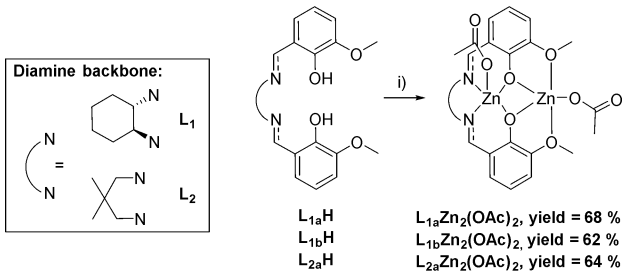

(i) 2 equiv of [$Zn(OAc)_2{\cdot}2(H_2O)$], MeOH, 22 °C, 16 h.

Crystals suitable for X-ray diffraction studies were obtained for $\mathbf{L_{1a}Zn_2(OAc)_2}$ by slow diffusion of pentane into a concentrated dichloromethane solution. The molecular structure of $\mathbf{L_{1a}Zn_2(OAc)_2}$ shows that both the zinc centers are pentacoordinated by the ligand framework (Figure 1 and Figure S9, Table 1); one within the "enclosed" phenolic pocket, and the other in the "open" cavity. A κ^2-coordinated acetate ligand provides stabilization for the dinuclear complex by bridging between the two Zn centers. The zinc center enclosed in the small pocket is coordinated via two nitrogen centers, two phenolic oxygen centers, and one acetate oxygen in a distorted square pyramidal geometry (τ = 0.16).[29] In contrast, the zinc occupying the open pocket has a distorted trigonal bipyramidal

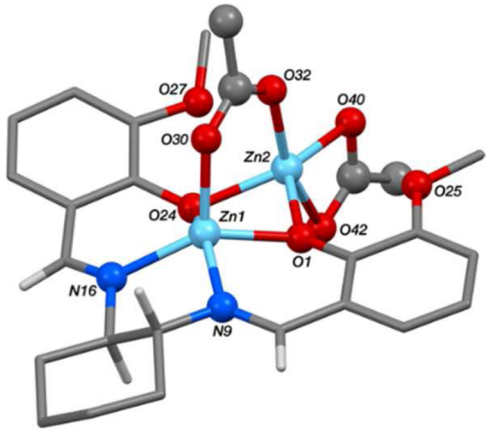

Figure 1. The crystal structure of $(\mathbf{L_{1a}})\mathbf{Zn_2(OAc)_2}$. Hydrogen atoms and a dichloromethane molecule are omitted for clarity.

DOI: 10.1021/acs.inorgchem.5b02233
Inorg. Chem. XXXX, XXX, XXX−XXX

Table 1. Selected Bond Lengths (Å) and Angles (deg) for $L_{1a}Zn_2(OAc)_2$

Zn(1)−O(1)	2.003(2)	Zn(1)−N(9)	2.027(3)
Zn(1)−N(16)	2.036(2)	Zn(1)−O(24)	2.023(2)
Zn(1)−O(30)	1.994(2)	Zn(2)−O(24)	2.021(2)
Zn(2)−O(1)	2.055(2)	Zn(2)−O(40)	2.096(2)
Zn(2)−O(32)	2.023(2)	Zn(2)−O(42)	2.192(2)
Zn(1)···Zn(2)	2.9539(4)	O(1)−Zn(1)−N(9)	90.03(9)
Zn(2)···O(25)	2.764(2)	O(30)−Zn(1)−N(16)	115.57(10)
Zn(2)···O(27)	2.592(2)	O(32)−Zn(2)−O(42)	161.27(9)

geometry (τ = 0.34) and is coordinated by two phenolic oxygen atoms, one bridging acetate oxygen, and a terminal κ^2 acetate. In the solid state, the two methoxy groups on the salen ligand do not coordinate to the zinc in the open pocket [Zn2−O25, 2.764(2) Å; Zn2−O27, 2.592(2) Å]. The distance between the two zinc centers is 2.9539(4) Å, which is small compared to other dinuclear catalysts (~3.1 Å).[10a,b,19] A similar molecular structure has been reported for the closely related hydrate complex, $L_{1a}Zn_2(OAc)_2{\cdot}H_2O$ (Figure S10), where the two zinc centers adopt distorted square pyramidal geometries.[30] The zinc center occupying the enclosed pocket of $L_{1a}Zn_2(OAc)_2{\cdot}H_2O$ has a similar coordination mode to that of $L_{1a}Zn_2(OAc)_2$. However, the zinc center in the open pocket is coordinated to just one phenolic oxygen, with one methoxy group, one water, and two acetate ligands (one bridging and one terminal) completing the coordination sphere of the second zinc. As a result, the Zn···Zn distance is longer [3.358(1) Å] but still in the range of common dinuclear catalysts for epoxide/CO_2 ROCOP.[10a,b,19] It is relevant to consider that the coordination of water by $L_{1a}Zn_2(OAc)_2{\cdot}H_2O$ indicates that the zinc coordination geometry within $L_{1a}Zn_2(OAc)_2$ is likely to be altered in the presence of a Lewis donor, suggesting that under the polymerization conditions, the epoxide (CHO) could coordinate to the zinc center in the open pocket. Furthermore, the different coordination geometries of the zinc in the open pocket suggest that the methoxy groups may play a role in stabilizing the active sites during the polymerization.

In the solution state, the ^{1}H NMR spectra of imine complexes $L_{1a}Zn_2(OAc)_2$ and $L_{2a}Zn_2(OAc)_2$ confirm the two metals are coordinated, with all the resonances experiencing upfield shifts in comparison to the free ligands (Figure S11−14). A particularly significant shift was observed for the imine signal in $CDCl_3$ [from 13.84 ppm in $L_{1a}H$ to 8.23 ppm for $L_{1a}Zn_2(OAc)_2$ (Figure S11) and from 14.14 ppm in $L_{2a}H$ to 8.08 ppm for $L_{2a}Zn_2(OAc)_2$ (Figure S13)]. The broadness of the methylene resonances and the loss of the phenolic proton resonance also confirm the deprotonation of the ligand and the coordination of a zinc center. The appearance of two new singlet resonances at 2.00 and 1.97 ppm are assigned to the two distinct acetate coligands. Similarly, the ^{1}H NMR spectrum of the amine complex $L_{1b}Zn_2(OAc)_2$ exhibits upfield resonances in comparison to those of the free ligand (Figures S15 and S16). In d_5-pyridine, it can be seen that the N−H resonances are broad (4.28 ppm) and that a significant shift of the benzylic resonance occurs (from 4.01 to 4.19 ppm), indicating that the zinc center is located within the small pocket. The acetate resonance at 2.11 ppm is assigned to both the zinc-coordinated acetate ligands. DOSY analysis of $L_{2a}Zn_2(OAc)_2$ in $CDCl_3$ (Figure S17) and of $L_{1b}Zn_2(OAc)_2$ in d_5-pyridine (Figure S18) shows that, in each case, all the ^{1}H NMR resonances possess the same diffusion coefficient and give a predicted molecular weight close to the theoretical one (456 g/mol for 614 g/mol and 729 g/mol for 633 g/mol, respectively), providing further confirmation of the dinuclear complex structures. To confirm the stability of $L_{2a}Zn_2(OAc)_2$ under typical polymerization conditions, $L_{2a}Zn_2(OAc)_2$ was heated to reflux for 16 h in d_8-THF. The ^{1}H NMR spectra remained constant over time, indicating that this species is thermally stable under the polymerization conditions (Figure S19). Unfortunately, this test could not be performed on $L_{1a}Zn_2(OAc)_2$ and $L_{1b}Zn_2(OAc)_2$ as they were not soluble even in hot THF.

In contrast to the other ligands, the direct reaction of $L_{2b}H$ with either $Zn(OAc)_2$ or $Zn(OAc)_2{\cdot}2(H_2O)$ gave a mixture of products (Scheme 3). Although the ^{1}H NMR spectrum in any

Scheme 3. Reactivity of $L_{2b}H$ with $Zn(OAc)_2{\cdot}2H_2O$ Giving Rise to a Mixture of Products Containing $L_{2b}Zn_2(OAc)_2$, $L_{2b}Zn_3(OAc)_4$, and $(L_{2b})_2Zn_3(OAc)_2$

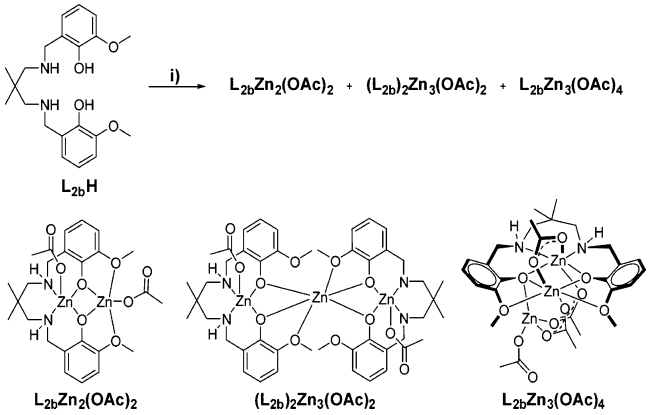

(i) 2 equiv of $Zn(OAc)_2{\cdot}2(H_2O)$, MeOH, 22 °C, 16 h.

solvent was convoluted (Figures S20 and S21), no signals corresponding to the free ligand were observed; instead, three new sets of resonances were present. MALDI-TOF analysis of the mixture revealed the presence of $L_{2b}Zn_2(OAc)_2$ (M^{+1}-OAc = 563 g/mol) along with two higher molecular weight species, assigned as $L_{2b}Zn_3(OAc)_4$ [($M_1{}^{+1}$-OAc = 745 g/mol) and $(L_{2b})_2Zn_3(OAc)_2$ ($M_2{}^{+1}$-OAc = 999 g/mol)] (Figure S22). DOSY analysis of the product mixture in C_6D_6 showed a range of diffusion coefficients [-9.1×10^{-10} m^2/s to -9.3×10^{-10} m^2/s)] (Figure S23). A comparison of the diffusion coefficients obtained from a calibration plot of known standards gave a predicted molecular weight range of 496 g/mol to 977 g/mol, which is in agreement with the presence of products $L_{2b}Zn_2(OAc)_2$ (621 g/mol), $L_{2b}Zn_3(OAc)_4$ (802 g/mol), and $(L_{2b})_2Zn_3(OAc)_2$ (1061 g/mol) in the solution state.

An alternative synthetic route was investigated using a stepwise procedure via the synthesis of a monometallic intermediate, $L_{2b}Zn$ (Scheme 4), followed by its reaction with $Zn(OAc)_2$, and was expected to afford the dinuclear complex $L_{2b}Zn_2(OAc)_2$ (Scheme 5). Accordingly, when $L_{2b}H$ was deprotonated, using either $Zn(OAc)_2$ or Et_2Zn in dry MeOH or THF, respectively, the formation of a white precipitate was observed. The solid-state structure of $L_{2b}Zn$ was determined as both the THF and methanol solvates (Figures S24−26). Although the two solvates are very distinct crystallographically (with the structure of the THF solvate containing one independent C_i-symmetric complex, whereas that of the methanol solvate contains two independent C_i-symmetric complexes), the conformations of all three

DOI: 10.1021/acs.inorgchem.5b02233
Inorg. Chem. XXXX, XXX, XXX−XXX

Scheme 4. Reaction of $L_{2b}H$ with 1 equiv of Et_2Zn and the Formation of the Dimeric Structure $(L_{2b})_2Zn_2$

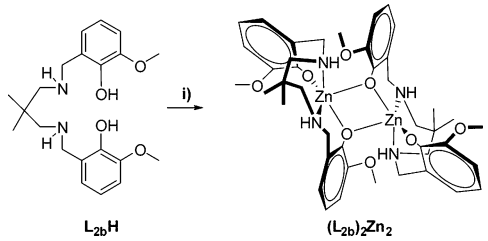

(i) 1 equiv of Et_2Zn in THF, 22 °C, 16 h or 1 equiv of $Zn(OAc)_2$ in MeOH, 22 °C, 16 h.

Scheme 5. Reaction of $(L_{2b})Zn_2$ with Et_2Zn and $Zn(OAc)_2$

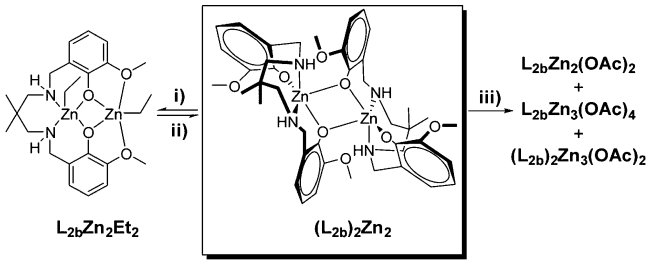

(i) 1 equiv of Et_2Zn in THF, 22 °C, 16 h (ii) 1 equiv of $L_{2b}H$ in C_6D_6. (iii) 1 equiv of $Zn(OAc)_2$ in THF, 22 °C, 16 h.

complexes are very similar. For simplicity, only the THF solvate will be discussed here, with full crystallographic details being provided in the Supporting Information. The molecular structure of $L_{2b}Zn$ reveals that it is dimeric and possesses C_i symmetry, with a central $\{Zn_2O_2\}$ ring, where one phenolic oxygen from each ligand bridges between the two zinc metal centers (Figure 2 and Table 2). The symmetry-related zinc centers adopt a trigonal bipyramidal geometry (τ = 0.70) and are bound to three phenolic oxygens in a fac fashion. The complexation of the zinc leads to the formation of six-membered rings, providing stabilization for the dimeric complex. The methoxy groups do not coordinate to zinc, and so the open pocket remains available for the coordination of another metal center. Multinuclear (^1H, ^{13}C) NMR spectroscopy along with two-dimensional (2D) NMR and DOSY experiments suggest that the dimeric structure is retained in solution (Figures S27−29)

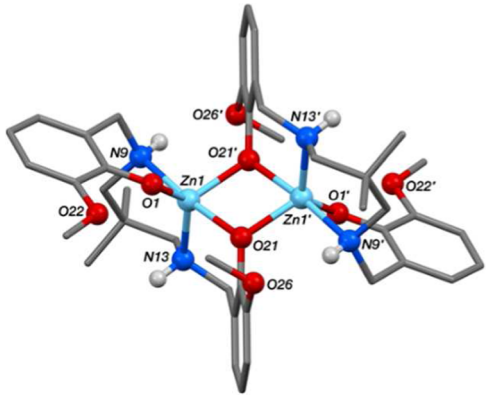

Figure 2. The crystal structure of $(L_{2b})_2Zn_2$-THF. Hydrogen atoms and three THF molecules are omitted for clarity.

Table 2. Selected Bond Lengths (Å) and Angles (deg) for $(L_{2b})_2Zn_2$

Zn(1)−O(1)	1.925(2)	O(1)−Zn(1)−N(13)	131.60(9)
Zn(1)−O(21′)	2.004(2)	O(1)−Zn(1)−O(21′)	116.99(8)
Zn(1)−O(21)	2.088(2)	O(21′)−Zn(1)−N(13)	110.84(8)
Zn(1)−N(9)	2.160(2)	O(21′)−Zn(1)−N(9)	173.79(7)
Zn(1)−N(13)	2.109(2)	O(21)−Zn(1)−N(13)	90.70(8)
C(20)−O(21)	1.336(3)	O(21′)−Zn(1)−O(21)	79.11(7)
Zn(1)···Zn(1)	3.1557(5)	O(1)−Zn(1)−O(21)	91.19(7)

To investigate whether the dimer $(L_{2b})_2Zn_2$ can be cleaved by the coordination of a second metal, the reaction of $(L_{2b})_2Zn_2$ with 1 equiv of Et_2Zn was performed (Scheme 5). This reaction was selected because reactions involving Et_2Zn are generally fast and because the formation of dinuclear complexes can be monitored by following the distinctive ^1H NMR signals of the Zn-ethyl groups. The ^1H NMR spectrum of the product, in C_6D_6, showed no trace of the unreacted dimer, and all resonances experienced an upfield shift, consistent with the incorporation of a second zinc center within the ligand scaffold (Figures S30 and S31). Two different sets of characteristic Zn-ethyl resonances are observed, with two triplets at 2.05 and 1.79 ppm and the corresponding quartets at 0.94 and 0.61 ppm. These Zn-ethyl chemical shifts are significantly different than those of diethylzinc [1.11 ppm (t) and 0.12 ppm (q) in C_6D_6],[31] confirming the coordination of the second zinc center within the ligand scaffold.

^1H DOSY NMR spectroscopy shows that all the resonances possess the same diffusion coefficient (Figure S32). The estimation of the molecular weight based on the diffusion coefficient, using a calibration plot, gave a calculated molecular weight of 503 g/mol, which is consistent with the formation of a monomeric $L_{2b}Zn_2Et_2$ product (561 g/mol). Nevertheless, block colorless crystals, obtained from a saturated THF solution of $L_{2b}Zn_2Et_2$ at 22 °C, corresponded to the starting dimer $(L_{2b})_2Zn_2$; this finding suggests that the second metal is weakly coordinated within the ligand scaffold and that an equilibrium exists between $L_{2b}Zn_2Et_2$, Et_2Zn, and $(L_{2b})_2Zn_2$. To emphasize the lability of the metal centers within this ligand system, 1 equiv of free ligand was added to a solution of $L_{2b}Zn_2Et_2$, in C_6D_6 (Scheme 5). The instantaneous formation of a precipitate was observed, with concomitant release of ethane. The white precipitate was isolated, dissolved in d_8-THF, and the resultant spectrum correspond to the dimer $(L_{2b})_2Zn_2$. Finally, when the dimer $(L_{2b})_2Zn_2$ was reacted with 1 equiv of $Zn(OAc)_2$ at room temperature, the same product mixture was obtained as when the parent ligand was reacted with 2 equiv of $Zn(OAc)_2$ (Scheme 5).

Further investigations were performed to quantify the ratio of the reaction products $L_{2b}Zn_2(OAc)_2$, $L_{2b}Zn_3(OAc)_4$, and $(L_{2b})_2Zn_3(OAc)_2$. Complexes $L_{2b}Zn_3(OAc)_4$ and $(L_{2b})_2Zn_3(OAc)_2$ were independently synthesized by the reaction of $L_{2b}H$ with 3 equiv or 1.5 equiv of $Zn(OAc)_2$ in THF, respectively (Scheme 6). Colorless block crystals of $L_{2b}Zn_3(OAc)_4$ suitable for X-ray diffraction were obtained by slow diffusion of pentane into a saturated dichloromethane solution of $L_{2b}Zn_3(OAc)_4$ (Figure 3, Table 3, and Figure S33). The molecular structure reveals that Zn1 and Zn2 each possess an octahedral coordination sphere, while Zn3 is tetrahedral. Zn1 occupies the enclosed phenolic pocket and is coordinated by both phenolic oxygen centers and both amine nitrogens, with two bridging acetate ligands completing its coordination sphere. Zn2 occupies the open phenolic pocket and is

DOI: 10.1021/acs.inorgchem.5b02233
Inorg. Chem. XXXX, XXX, XXX−XXX

Scheme 6. Reaction of $L_{2b}H$ with (i) 1.5 equiv and (ii) 3 equiv of $Zn(OAc)_2$

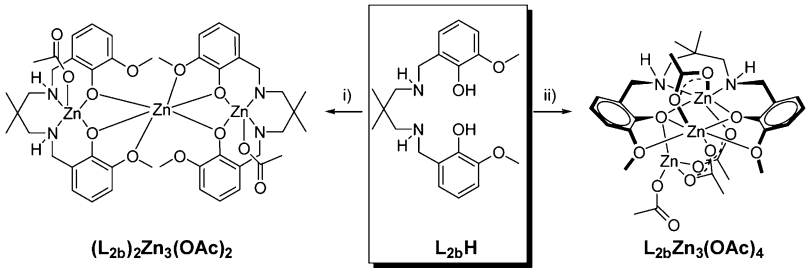

(i) 1.5 equiv of $Zn(OAc)_2$ in THF, 22 °C, 16 h; (ii) 3 equiv of $Zn(OAc)_2$ in THF, 22 °C, 16 h.

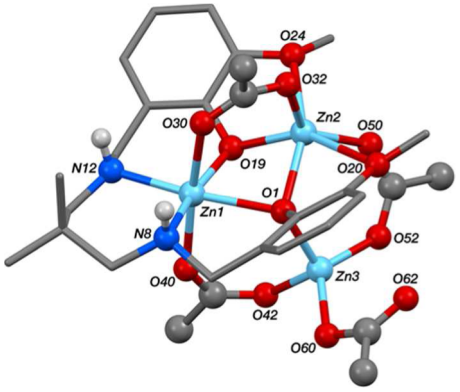

Figure 3. The crystal structure of $(L_{2b})Zn_3(OAc)_4$. Hydrogen atoms omitted for clarity.

Table 3. Selected Bond Lengths (Å) of $L_{2b}Zn_3(OAc)_4$

Zn(1)–O(1)	2.241(3)	Zn(2)–O(1)	2.139(4)
Zn(1)–O(19)	2.043(4)	Zn(2)–O(20)	2.576(4)
Zn(1)–O(30)	2.191(4)	Zn(2)–O(24)	2.330(4)
Zn(1)–N(8)	2.087(5)	Zn(2)–O(32)	1.950(4)
Zn(1)–N(12)	2.095(4)	Zn(3)–O(1)	2.005(3)
Zn(2)–O(19)	1.994(4)	Zn(3)···Zn(2)	3.2936(9)
Zn(1)···Zn(2)	3.0546(9)	Zn(3)···Zn(1)	3.6005(8)

coordinated by both methoxy groups, although the bond distance is quite long [Zn2–O24, 2.330(4) Å and Zn2–O20, 2.576(4) Å], with two bridging acetate ligands providing further stabilization. Zn3 is only coordinated to one phenolic oxygen and is coordinated to the other zinc centers via two κ^2-bridging acetate ligands, with coordination by an additional, terminal acetate ligand. The ligand adopts a bowl shape and has a very similar structure to the related trizinc complex coordinated by a bis(phenolate) tetra(amine) macrocycle.[11f] The ^{1}H NMR spectrum of $L_{2b}Zn_3(OAc)_4$ is consistent with the formation of a trizinc complex (Figure S34). Although the acetate resonance overlaps with the NH and methylene ligand resonances, the integration gives good agreement with the presence of four acetate coligands coordinated to the metal centers. In addition, the DOSY spectrum shows that all the resonances possess the same diffusion coefficient, suggesting that the trizinc structure is retained in C_6D_6 solution (Figure S36). The estimation of the complex molecular weight, based on the diffusion coefficient, gave a calculated molecular weight of 725 g/mol, which is in close agreement with the calculated value (802 g/mol). The product is also stable, under reflux conditions in THF solution, over a period of 16 h (Figure S37). The reaction of 1.5 equiv of $Zn(OAc)_2$ with $L_{2b}H$ gave a convoluted ^{1}H NMR spectrum in C_6D_6 (Figure S38). No signals from the unreacted ligand, dimer $(L_{2b})_2Zn_2$, or the trimetallic species $L_{2b}Zn_3(OAc)_4$ were observed, suggesting that a new product is formed. DOSY spectroscopy reveals that the new resonances all possess the same diffusion coefficient (Figure S39), corresponding to a molecular weight of 978 g/mol, which is in close agreement with the value for $(L_{2b})_2Zn_3(OAc)_2$ (1063 g/mol). Although crystals of $(L_{2b})_2Zn_3(OAc)_2$ suitable for X-ray diffraction experiments could not be obtained, it was possible to grow crystals for the closely related trizinc bis(chloride) complex, $(L_{2b})_2Zn_3Cl_2$ (Figure S40), providing further support for the formation of a trizinc complex coordinated by the ancillary ligands.[32]

Table 4. Copolymerization[a] of CO_2 and CHO at 1 bar of CO_2

entry	catalyst	TON[b]	TOF[c] (h^{-1})	% carbonate[d]	% selectivity[d]	M_n[e], (g/mol^{-1})	$Đ$[e]	time
1	$L_{1a}Zn_2(OAc)_2$	15	0.2	71	84	400	1.09	4 d
2	$L_{1b}Zn_2(OAc)_2$	14	0.1	77	83	400	1.10	4 d
3	$L_{2a}Zn_2(OAc)_2$	45	2	>99	87	1500	1.3	1 d
4	$L_{2b}Zn_2(OAc)_2$ **mix**	9	2	>99	80	-	-	4.5 h
5	$L_{2b}Zn_2(OAc)_2$ **mix**	30	0.3	88	82	1000	1.17	4 d
6	$L_{2b}Zn_3(OAc)_4$[f]	19	3	45	92	-	-	6 h
7	$L_{2b}Zn_3(OAc)_4$[f]	24	1	52	93	-	-	24 h
8	$(L_{2b})_2Zn_3(OAc)_2$	23	1	85	77	400	1.17	1 d
9	dizinc macrocycle catalyst[11f,g]	99	17	>99	>99	1300	1.23	6 h
10	trizinc macrocycle catalyst[11f,g]	96	4	>99	97	3400	1.21	1 d

[a]Copolymerization conditions: catalyst/CHO = 1 mol %, 80 °C, 1 bar of CO_2. [b]TON = number of moles of epoxide consumed per mole of catalyst. [c]TOF = TON/h. [d]Determined by comparison of the integrals of signals arising from the methylene protons in the ^{1}H NMR spectra due to copolymer carbonate linkages (δ = 4.65 pmm), copolymer ether linkages (δ = 3.45 ppm), and the signals due to the cyclic carbonate byproduct (δ = 4.00 ppm). [e]Determined by SEC in THF calibrated using polystyrene standards. [f]Catalyst/CHO = 0.5 mol %. [g]Catalyst/CHO = 0.1 mol %.

DOI: 10.1021/acs.inorgchem.5b02233
Inorg. Chem. XXXX, XXX, XXX–XXX

Comparison of ^{1}H NMR spectra of $\mathbf{L_{2b}Zn_3(OAc)_4}$ and $\mathbf{(L_{2b})_2Zn_3(OAc)_2}$ with the spectrum of products obtained from the reaction of $\mathbf{L_{2b}H}$ with 2 equiv of $Zn(OAc)_2{\cdot}2(H_2O)$ suggests that $\mathbf{L_{2b}Zn_3(OAc)_4}$ and $\mathbf{(L_{2b})_2Zn_3(OAc)_2}$ are the two major products (Figure S41). DOSY spectroscopy of the mixture provides further support for this observation, as two major species are observed with diffusion coefficients that correspond exactly to the values obtained for the independently prepared complexes $\mathbf{L_{2b}Zn_3(OAc)_4}$ and $\mathbf{(L_{2b})_2Zn_3(OAc)_2}$ (Figures S23, S36, and S39). A third product is also present, albeit in very low concentration, which is likely to be the dinuclear complex $\mathbf{L_{2b}Zn_2(OAc)_2}$. These findings suggest that using this ligand, the formation of the dinuclear complex is not favorable and that metal rearrangement occurs to form $\mathbf{L_{2b}Zn_3(OAc)_4}$ and $\mathbf{(L_{2b})_2Zn_3(OAc)_2}$. This was further supported as $\mathbf{L_{2b}Zn_3(OAc)_2}$ was isolated as a white precipitate from the reaction of $\mathbf{L_{2b}H}$ and 2 equiv of $Zn(OAc)_2$ in dry THF at −78 °C. As the dinuclear complex could not be isolated, the $\mathbf{L_{2b}Zn_2(OAc)_2}$ mixture, $\mathbf{L_{2b}Zn_3(OAc)_4}$, and $\mathbf{(L_{2b})_2Zn_3(OAc)_2}$ were each tested within polymerization studies.

Polymerization Catalysis. The series of dizinc complexes were tested as catalysts for the ROCOP of CO_2 and CHO, at 1 bar of pressure of CO_2 and 80 °C (Table 4). As other dizinc catalysts are active under these conditions, the reaction provides a useful benchmark for comparison.[11f,13a,18] All catalysts displayed a low activity; therefore, high catalyst loadings were required to convert CHO and CO_2 to PCHC. In particular, complexes containing the $\mathbf{L_1}$ ligand backbone [$\mathbf{L_{1a}Zn_2(OAc)_2}$, and $\mathbf{L_{1b}Zn_2(OAc)_2}$] showed negligable TOF values (~0.1 h^{-1}; Entries 1 and 2) at a catalyst loading of 1 mol % versus CHO. These low activities are attributed to the poor solubility of the catalyst in CHO. With the $\mathbf{L_2}$ backbone, the $\mathbf{L_{2b}Zn_2(OAc)_2}$ mixture displayed improved solubility in hot CHO and showed slightly higher TOF values of 2 h^{-1} (Entry 4). However, after the first 4.5 h of reaction, a white precipitate formed, and the TOF decreased to 0.3 h^{-1}. Similarly, $\mathbf{L_{2b}Zn_3(OAc)_4}$ was active during the first 6 h of polymerization (TOF = 3 h^{-1}, Entry 6) with similar activity to that of the trizinc macrocycle catalyst reported previously (Entry 10);[11f] however, the polymers have only low carbonate linkage content, with 45% of ether linkages. Again, formation of a white precipitate was observed after 6 h, and the activity of the catalyst decreased (TOF 1 h^{-1} after 24 h, Entry 7). The white solid was isolated, and its ^{1}H NMR spectrum showed catalyst decomposition (Figure S42). This observation suggests that the trizinc complex $\mathbf{L_{2b}Zn_3(OAc)_4}$ decomposes during the polymerization reaction, most likely to form the dimer $\mathbf{(L_{2b})_2Zn_2}$ and $Zn(OAc)_2$, which could explain the low activity observed. Under these conditions, the catalysts could only produce oligomers with low molecular weights. However, slightly higher activities (TOF of 2 and 1 h^{-1}) were obtained with the more stable $\mathbf{L_{2a}Zn_2(OAc)_2}$ (Entry 3) and $\mathbf{(L_{2b})_2Zn_3(OAc)_2}$ (Entry 8). The imine complex $\mathbf{L_{2a}Zn_2(OAc)_2}$ also showed an improved CO_2 uptake compared to the rest of the series, producing almost perfectly alternating copolymers of low molecular weight (1500 g/mol). Despite the low activities recorded for all the catalysts, the observations from this set of experiments suggest that complexes containing the $\mathbf{L_1}$ backbone tend to have lower activity compared to those with the $\mathbf{L_2}$ backbone, probably due to their lack of solubility in neat CHO at high loadings.

Previously, it has been reported that some dizinc complexes show activities that are dependent on the CO_2 pressure; indeed, such effects were usually observed for complexes coordinated by flexible ligands.[17] Therefore, the catalysts were also tested at 30 bar of CO_2 pressure. In all cases, an improvement in the catalytic activity was observed, as all the complexes produced PCHC at much lower catalyst loading (0.1 mol % catalyst vs CHO). On the one hand, the activity of $\mathbf{L_{1a}Zn_2(OAc)_2}$, $\mathbf{L_{1b}Zn_2(OAc)_2}$, the $\mathbf{L_{2b}Zn_2(OAc)_2}$ mixture, and $\mathbf{(L_{2b})_2Zn_3(OAc)_2}$ were still very low (Table 5, Entries 1, 2, 4, and 6, respectively). On the other hand, $\mathbf{L_{2a}Zn_2(OAc)_2}$ (Entry 3) and $\mathbf{L_{2b}Zn_3(OAc)_4}$ (Entry 5) showed a significant enhancement in their catalytic activities (TOF = 44 and 9 h^{-1}, respectively) and polymer selectivities. The best catalyst, $\mathbf{L_{2a}Zn_2(OAc)_2}$, has comparable activity to other metal salen catalysts[4g,20e] and to the dinickel salen complex that was previously reported by Ko and co-workers (TOF = 56 h^{-1}).[26] At 80 °C, $\mathbf{L_{2a}Zn_2(OAc)_2}$ formed PCHC with a very high carbonate linkage content and with much better polymer selectivities (M_n = 18 800 g/mol, $Đ$ = 1.6). These results show that the more flexible $\mathbf{L_2}$ backbone gave catalysts with higher activity than those with the $\mathbf{L_1}$ backbone.

Table 5. Copolymerization[a] of CO_2 and CHO at 30 bar of CO_2

entry	catalyst	TON[b]	TOF[c] (h^{-1})	% carbonate[d]	% selectivity[d]
1	$\mathbf{L_{1a}Zn_2(OAc)_2}$	34	2	>99	98
2	$\mathbf{L_{1b}Zn_2(OAc)_2}$	16	1	>99	89
3	$\mathbf{L_{2a}Zn_2(OAc)_2}$	706	44	>99	94
4	$\mathbf{L_{2b}Zn_2(OAc)_2}$ mix	29	2	>99	94
5	$\mathbf{L_{2b}Zn_3(OAc)_4}$	147	9	75	87
6	$\mathbf{(L_{2b})_2Zn_3(OAc)_2}$	28	2	>99	89

[a]Copolymerization conditions: catalyst/CHO = 0.1 mol %, 80 °C, 30 bar of CO_2, 16 h. [b]TON = number of mole of epoxide consumed per mole of catalyst. [c]TOF = TON/h. [d]Determined by comparison of the integrals of signals arising from the methylene protons in the ^{1}H NMR spectra due to copolymer carbonate linkages (δ = 4.65 pmm), copolymer ether linkages of moles of epoxide (δ = 3.45 ppm), and the signals due to the cyclic carbonate byproduct (δ = 4.00 ppm).[11g]

The series of catalysts was also tested for the ROCOP of PA and CHO. In 2014, Lu et al. reported that $\mathbf{L_{1a}Zn_2(OAc)_2{\cdot}H_2O}$ could polymerize maleic anhydride and CHO when a cocatalyst such as *N*,*N*-dimethylaminopyridine was present.[30] In this case, all the catalysts could fully polymerize PA, in 16 h, without the need for a cocatalyst (Table 6). While the imine complexes afforded the corresponding polyesters (PE) with high selectivity and no ether linkages, the amine complexes provided the polymers with a greater proportion of ether linkages. A possible explanation for this trend is that the more electron-donating imine decreases the Lewis acidity of the metal center, thereby decreasing the likelihood of successive ring opening two CHO molecules. Comparing the catalyst activities, $\mathbf{L_{1a}Zn_2(OAc)_2}$ (Entry 1) gave activities (TOF = 70 h^{-1}) similar to some of the best catalysts based on chromium, cobalt, or aluminum salen/salophen complexes,[16a] all of which require the use of a cocatalyst. However, $\mathbf{L_{2a}Zn_2(OAc)_2}$ (Entry 3) was significantly more active (TOF = 198 h^{-1}) than the majority of other known catalysts for this reaction, under similar conditions.[33] Both

DOI: 10.1021/acs.inorgchem.5b02233
Inorg. Chem. XXXX, XXX, XXX−XXX

Table 6. Copolymerization of PA[a] and CHO

entry	catalyst	conv [%][b]	TON[c]	TOF[d] (h^{-1})	% ester[e]	time	M_n[f], (g mol^{-1})	$Đ$[f]
1	$L_{1a}Zn_2(OAc)_2$	70	70	70	>99	1 h	4400	1.15
2	$L_{1b}Zn_2(OAc)_2$	64	64	11	27	6 h	6400	2.18
3	$L_{2a}Zn_2(OAc)_2$	99	99	198	>99	30 min	5300	1.23
4	$L_{2b}Zn_2(OAc)_2$ mix	59	59	10	21	6 h	8200	2.17
5	$L_{2b}Zn_3(OAc)_4$	28	28	28	13	1 h	7400	2.75
6	$(L_{2b})_2Zn_3(OAc)_2$	61	61	10	26	6 h	7700	2.24

[a]Copolymerization conditions: catalyst/PA/CHO = 1/100/800, 100 °C. [b]Determined by ^{1}H NMR spectroscopy (deuterated dimethyl sulfoxide (DMSO-d_6)) by integrating the normalized resonances for PA (7.97 ppm) and the phenylene signals in polyester (7.30−7.83 ppm). [c]TON = number of moles of epoxide consumed per mole of catalyst. [d]TOF = TON/h. [e]Determined by ^{1}H NMR spectroscopy (DMSO-d_6) by integrating the normalized resonances for ester linkages (4.80−5.26 ppm) and ether linkages (3.22−3.64 ppm). [f]Determined by SEC in THF calibrated using polystyrene standards.

$L_{1a}Zn_2(OAc)_2$ and $L_{2a}Zn_2(OAc)_2$ afford polymers with high ester linkages and with narrow dispersities.

Terpolymerization of PA/CHO/CO_2. The promising results of $L_{2a}Zn_2(OAc)_2$ toward CHO/CO_2 and PA/CHO ROCOP prompted the investigation of the terpolymerization of PA/CHO/CO_2. The reaction was performed at 100 °C and 30 bar of CO_2 pressure with a 100/1000 mixture of PA/CHO. The reaction was monitored by taking aliquots after 2 and 18 h. After 2 h, ^{1}H NMR analysis showed selective polyester formation, with the appearance of a distinctive resonance at 5.06 ppm (74% conversion) and with no traces of PCHC observed (Figure S43). ^{1}H NMR analysis after 18 h showed full conversion of PA (with loss of the resonances at 7.84 and 7.95 ppm) and the formation of PCHC, shown by the increase of intensity of the resonance at 4.64 ppm. Between 2 and 18 h, a clear increase in the molecular weight was observed, from 3598 to 7085 g/mol, along with conservation of the polydispersity index (1.20). ^{13}C NMR and DOSY analysis of the crude polymer suggests that the PE and PCHC blocks are connected, as only two carbon signal can be found in the carbonate region (162.7 and 166.6 ppm); both sets of resonances have a diffusion coefficient of -9.81×10^{-10} m^2/s (Figures S44 and S45). This evidence suggests that $L_{2a}Zn_2(OAc)_2$ can be used to synthesize poly(ester-*block*-carbonates) from a one-pot reaction through a PA/CHO/CO_2 terpolymerization.

CONCLUSIONS

A series of dinuclear zinc salen complexes that are active catalysts for carbon dioxide/cyclohexene oxide and phthalic anhydride/cyclohexene oxide ROCOP were investigated. These studies highlight the influence of the ligand structures on the catalytic activity and the stability of the dinuclear complexes. Ligands containing imine moieties resulted in complexes that were more stable than the amine analogues. Consequently, a mixture of products, deriving from metal disproportionation, was obtained with the more flexible amine $L_{2b}H$ ligand, highlighting its complex solution coordination chemistry. The catalytic studies indicate that complexes with the more flexible 2,2-dimethyl propylene backbones are more active than those with the *trans*-1,2-cyclohexylene backbones. Further, the complexes with imine substituents showed much better selectivities, affording perfectly alternating copolymers, whereas complexes with amine substitutents gave higher ether-linkage content. The best catalyst, $L_{2a}Zn_2(OAc)_2$, combines imine donors with a flexible 2,2-dimethyl propylene backbone. It shows higher activity than other dizinc salen catalysts for carbon dioxide/CHO copolymerizations and higher activities than other reported catalysts for PA/CHO copolymerizations. $L_{2a}Zn_2(OAc)_2$ was also used to successfully afford poly(ester-*block*-carbonate) from the one-pot terpolymerization of PA/CO_2/CHO, providing further evidence that this simple system is selective and is able to synthesize polymers with more complicated structures.

EXPERIMENTAL SECTION

All solvents and reagents were obtained from commercial sources (Aldrich and Merck) and used as received unless stated otherwise. The solvents THF, toluene, and hexane were predried over activated molecular sieves (THF) or potassium hydroxide (toluene and hexane) then refluxed over sodium/benzophenone. All dry solvents and reagents were stored under nitrogen and degassed by several freeze−pump−thaw cycles. When stated, manipulations were performed using a double-manifold Schlenk vacuum line under nitrogen atmosphere or a nitrogen-filled glovebox. Cyclohexene oxide was dried over calcium hydride, filtered, purified by fractional distillation prior to use, and stored under an inert nitrogen atmosphere. Phthalic anhydride was purified by dissolving in benzene, filtering off impurities, recrystallizing from chloroform, and then subliming. Research-grade carbon dioxide was used for copolymerization studies.

NMR. ^{1}H, ^{13}C, and 2D NMR (COSY, HMQC) spectra were recorded using a Bruker AV 400 MHz spectrometer at 298 K (unless otherwise stated). DOSY analysis was performed using a Bruker AV 500 MHz spectrometer at 298 K (see the DOSY NMR section in the Supporting Information for more details).

MALDI-TOF MS. MALDI TOF analysis was performed on Micromass MALDI micro MX spectrometer. The matrix used was *trans*-2-[3-(4-*tert*-butylphenyl)-2-methyl-2-propenylidene]-malononitrile, and sodium acetate was used as an additive, when necessary. The samples were prepared as follows: 10 mg/mL THF solutions of the complex, matrix, and additive were separately prepared. Then, 20 μL of the complex and 20 μL of the matrix solution were mixed, along with 10 μL of the additive solution, if required. This mixture (2 μL) was then spotted on the MALDI plate and allowed to dry.

X-ray Diffraction. Data were collected using an Agilent Xcalibur 3E diffractometer, and the structures were refined using the SHELXTL and SHELX-2013 program systems. The crystallographic data table of all the compounds can be found in the Supporting Information (Table S4).

Elemental Analysis. Elemental analysis was determined by Stephen Boyer at London Metropolitan University.

Size-Exclusion Chromatography. Two Mixed Bed PSS SDV linear S columns were used in series, with THF as the eluent, at a flow rate of 1 mL/min, on a Shimadzu LC-20AD instrument at 40 °C. Polymer molecular weight (M_n) was determined by comparison against polystyrene standards. The polymer samples were dissolved in SEC-grade THF and filtered prior to analysis.

Typical Procedure for the Amination of *o*-Vanillin ($L_{1a}H$ and $L_{2a}H$). The appropriate diamine [(±)-*trans*-1,2-diaminocyclohexane (1.87 g, 0.016 mol) or 2,2-dimethyl-1,3-propanediamine (1.67 g, 0.016 mol)] in MeOH (5 mL) was added dropwise to a pale yellow solution

DOI: 10.1021/acs.inorgchem.5b02233
Inorg. Chem. XXXX, XXX, XXX−XXX

of *o*-vanillin (5 g, 0.033 mol) in MeOH (50 mL). Upon addition of the diamine, a deep yellow solution was obtained. The mixture was stirred for 4 h at 22 °C, and the solvent was subsequently removed under vacuum to give a yellow powder. (Yields: $\mathbf{L_{1a}H}$: 6.1 g, 100% and $\mathbf{L_{2a}H}$: 5.9 g, 100%). ^{1}H and ^{13}C NMR spectra are in accordance with reported literature values.[30,34]

$\mathbf{L_{1a}H}$: Elemental analysis for $C_{22}H_{26}N_2O_4$ (382.86 g/mol): Calculated: C, 69.09; H, 6.85; N 7.32%. Found: C, 69.21; H, 6.93; N, 7.38%.

$\mathbf{L_{2a}H}$: Elemental analysis for $C_{21}H_{26}N_2O_4$ (370.49 g/mol): Calculated: C, 68.09; H, 7.07; N, 7.56%. Found: C, 68.21; H, 6.99; N, 7.45%.

Typical Reduction Procedure for the Synthesis of $\mathbf{L_{1b}H}$ and $\mathbf{L_{2b}H}$. The reduction was performed in situ following the synthesis of $\mathbf{L_{1a}H}$ or $\mathbf{L_{2a}H}$ in methanol solution, by slow addition of 3.5 equiv of $NaBH_4$ (***Caution!*** *Exothermic*). The reaction mixture was stirred for 2 h at 22 °C. Water was then added until a white precipitate was obtained. The suspension was left to stir for 16 h before the product was isolated via filtration as a white powder. (Yields: $\mathbf{L_{1b}H}$, 6.0 g, 97% and $\mathbf{L_{2b}H}$, 6.0 g, 97%)

$\mathbf{L_{1b}H}$: ^{1}H NMR (400 MHz, $CDCl_3$, 298 K) δ 6.78 (dd, 2H, J = 8.1, 1.6 Hz, *m*-Ph), 6.72 (t, J = 7.5 Hz, 2H, *p*-Ph), 6.63 (dd, J = 7.5, 1.6 Hz, 2H, *m*-Ph), 4.01 (d, J = 13.6 Hz, 2H, NH−CH_2-Ph), 3.88 (d, J = 13.6 Hz, 2H, NH−CH_2-Ph), 3.85 (s, 6H, O−CH_3), 2.40 (m, CH-cyclohexyl), 2.11 (m, 2H, CH_2−cyclohexyl), 1.67 (m, 2H, CH_2−cyclohexyl), 1.20 (m, 4H, CH_2−cyclohexyl). ^{13}C NMR (101 MHz, $CDCl_3$, 298 K) δ 147.9 (*i*-Ph), 146.8 (*o*-Ph), 124.1 (*o*-Ph), 120.7 (*m*-Ph), 118.9 (*p*-Ph), 110.8 (*m*-Ph), 60.5 (CH chiral-cyclohexyl), 56.0 (O−CH_3), 49.1 (C−CH_2-NH), 30.6 (CH_2−cyclohexyl), 24.3 (CH_2−cyclohexyl). *m*/*z* (ES): 387 ([$\mathbf{L_{1b}H}$ + H]$^+$, 100%). Elemental analysis for $C_{22}H_{30}N_2O_4$ (386.49 g/mol): Calculated: C, 68.37; H, 7.82; N, 7.18%. Found: C, 68.23; H, 7.91; N, 7.16%.

$\mathbf{L_{2b}H}$: ^{1}H NMR (400 MHz, $CDCl_3$, 298 K) δ 6.84 (dd, J = 7.5, 1.6 Hz, 2H, *m*-Ph), 6.75 (t, J = 7.8 Hz, 2H, *p*-Ph), 6.65 (dd, J = 7.5 Hz, 1.6 Hz, 2H, *m*-Ph), 4.79 (s, 4H, NH, and Ph−OH), 3.98 (s, 4H, NH−CH_2-Ph), 3.87 (s, 6H, O−CH_3), 2.56 (s, 4H, NH−CH_2−C), 1.00 (s, 6H, C-(CH_3)). ^{13}C NMR (101 MHz, $CDCl_3$, 298 K) δ 148.1 (*i*-Ph), 147.2 (*o*-Ph), 123.1 (*o*-Ph), 120.6 (*m*-Ph), 118.8 (*p*-Ph), 111.0 (*m*-Ph), 57.7 (C-CH_2−NH), 55.9 (O−CH_3), 53.2 (NH-CH_2−Ph), 34.7 ((CH_3)$_2$-*C*-(CH_2)$_2$), 24.4 (C-(CH_3)$_2$). *m*/*z* (ES): 375 ([$\mathbf{L_{2b}H}$ + H]$^+$, 100%). Elemental analysis for $C_{21}H_{30}N_2O_4$ (374.48 g/mol): Calculated: C, 67.35; H, 8.078; N 7.48%. Found: C, 67.19; H, 7.90; N 7.49%.

Synthesis of $\mathbf{L_{1a}Zn_2(OAc)_2}$ and $\mathbf{L_{1b}Zn_2(OAc)_2}$. A solution of $Zn(OAc)_2{\cdot}2(H_2O)$ (2 equiv) in MeOH (15 mL) was added in one portion into a solution of $\mathbf{L_{1a}H}$ or $\mathbf{L_{1b}H}$ (500 mg) in MeOH (3 mL). The reaction mixture was stirred at 22 °C for 16 h. The dizinc complexes $\mathbf{L_{1a}Zn_2(OAc)_2}$ and $\mathbf{L_{1b}Zn_2(OAc)_2}$ were isolated as a white powder via filtration (yields: $\mathbf{L_{1a}Zn_2(OAc)_2}$: 65%, 398 mg and $\mathbf{L_{1b}Zn_2(OAc)_2}$: 62%, 506 mg).

$\mathbf{L_{1a}Zn_2(OAc)_2}$: ^{1}H NMR (400 MHz, $CDCl_3$, 298 K) δ 8.23 (s, 2H, CH═N), 6.84 (d, J = 7.5 Hz, 2H, *m*-Ph), 6.79 (d, J = 8.2 Hz, 2H, *m*-Ph), 6.60 (t, J = 7.8 Hz, 2H, *p*-Ph), 3.88 (s, 6H, O−CH_3), 3.35 (br m, 2H, CH chiral cyclohexyl), 2.43 (br m, 2H, CH_2−cyclohexyl), 2.00 (br m, 6H OAc and 2H CH_2−cyclohexyl), 1.46 (br m, 4H, CH_2−cyclohexyl). ^{13}C NMR (101 MHz, $CDCl_3$) δ 165.4 (HC═N), 150.8 (*i*-Ph), 126.2 (*m*-Ph), 119.2 (*o*-Ph), 115.0 (*p*-Ph), 113.5 (*m*-Ph), 110.1 (*o*-Ph), 65.6 (CH-cyclohexyl), 55.7 (O−CH_3), 27.9 (CH_2−cyclohexyl), 24.4 (CH_2−cyclohexyl), 22.9 (OAc). Elemental analysis for $C_{26}H_{30}N_2O_8Zn_2$ (629 g/mol): Calculated: C, 49.62; H, 4.81; N, 4.45%. Found: C, 49.50; H, 4.89; N, 4.55%.

$\mathbf{L_{1b}Zn_2(OAc)_2}$: ^{1}H NMR (400 MHz, d_5-pyr, 298 K) δ 6.75 (m, 4H, *m*-Ph), 6.61 (t, J = 7.7 Hz, 2H, *p*-Ph), 4.28 (br s, 4H, NH−CH_2-Ph, and NH), 4.19 (br s, 2H, NH−CH_2-Ph), 3.60 (s, 6H, O−CH_3), 2.63 (s, 2H, chiral cyclohexyl), 2.32 (m, 2H, CH_2−cyclohexyl), 2.09 (s, 11H, OAc + HOAc), 1.60 (s, 2H, CH_2−cyclohexyl), 1.09 (m, 4H, CH_2−cyclohexyl). ^{13}C NMR (101 MHz, d_5-pyr, 298 K) δ 176.1 (*i*-Ph), 153.4 (*o*-Ph), 150.1 (*o*-Ph), 122.8 (*m*-Ph), 115.1 (*p*-Ph), 110.4 (*m*-Ph), 59.7 (chiral CH-cyclohexyl), 54.9 (O−CH_3), 50.3 (NH-CH_2−Ph), 29.9 (CH_2−cyclohexyl), 24.9 (CH_2−cyclohexyl), 22.3 (OAc). Elemental analysis for $C_{26}H_{34}N_2O_8Zn_2$ (633 g/mol): Calculated: C, 49.31; H, 5.41; N, 4.42%. Found: C, 49.18; H, 5.34; N, 4.39%.

Synthesis of $\mathbf{L_{2a}Zn_2(OAc)_2}$. A solution of $Zn(OAc)_2{\cdot}2(H_2O)$ (440 mg, 2 mmol) in MeOH (15 mL) was added to a solution of $\mathbf{L_{2a}H}$ (370 mg, 1 mmol) in MeOH (3 mL), and the reaction mixture was stirred at 22 °C for 16 h. After removal of all volatiles in vacuo, $\mathbf{L_{2a}Zn_2(OAc)_2}$ was isolated as a yellow powder. The pure product was obtained after washing with pentane followed by crystallization from THF/pentane at −40 °C (yield: 68%, 420 mg).

^{1}H NMR (400 MHz, $CDCl_3$, 298 K) δ 8.08 (s, 2H, N═CH), 6.84 (d, J = 7.9 Hz, 2H, *m*-Ph), 6.74 (dd, J = 8.0 Hz, 1.7 Hz, 2H, *m*-Ph), 6.60 (t, J = 7.8 Hz, 2H, *p*-Ph), 3.87 (s, 6H, O−CH_3), 3.72 (s, 4H, N−CH_2-C), 1.97 (s, 6H, OAc), 1.05 (s, 6H, C-(CH_3)$_2$). ^{13}C NMR (101 MHz, $CDCl_3$, 298 K) δ 171.1 (CH═N), 150.4 (*i*-Ph), 126.4 (*m*-Ph), 118.1 (*o*-Ph), 115.1 (*p*-Ph), 113.8 (*m*-Ph), 74.7 (CH═N), 55.9 (O−CH_3), 35.3 ((CH_2)$_2$−C-(CH_3)$_2$), 24.8 (C-(CH_3)$_2$), 23.0 (N-CH_2−C). Elemental analysis for $C_{25}H_{30}N_2O_8Zn_2$ (617 g/mol): Calculated: C, 48.64; H, 4.90; N 4.54%. Found: C, 48.66; H, 5.03; N, 4.43%.

Synthesis of $\mathbf{(L_{2b})_2Zn_2}$. Under a nitrogen atmosphere, $\mathbf{L_{2b}H}$ (1 g, 2.64 mmol) was dissolved in dry THF (35 mL). Subsequently, $ZnEt_2$ (326 mg, 2.64 mmol) was dissolved in dry THF (5 mL) and added dropwise into the ligand solution. The reaction mixture was then stirred at 22 °C for 16 h. $\mathbf{(L_{2b})_2Zn_2}$ was isolated via canular transfer of the solvent as a white powder (yield: 62%, 726 mg).

^{1}H NMR (400 MHz, d_8-THF, 298 K) δ 6.98 (dd, J = 7.9, 1.7 Hz, 1H, *m*-Ph), 6.83 (dd, J = 7.5, 1.8 Hz, 1H, *m*-Ph), 6.50 (t, J = 7.7 Hz, 1H, *p*-Ph), 6.46 (dd, J = 7.8, 1.7 Hz, 1H, *m*-Ph), 6.21 (dd, J = 7.5, 1.7 Hz, 1H, *m*-Ph), 6.03 (t, J = 7.6 Hz, 1H, *p*-Ph), 4.90 (t, J = 11.6 Hz, 1H, Ph−C*H*H-NH), 4.37 (s, 3H, O−CH_3), 3.82−3.65 (m, 2H, C*H*H-NH + N*H*), 3.50 (s, 3H, O−CH_3), 3.38 (t, J = 14.5, 11.9, 1.9 Hz, 2H, Ph−CH*H*-NH + NH−C*H*H-C), 3.08−2.84 (m, 2H, NH−C*H*H-C + NH), 2.56−2.43 (m, 1H, Ph−CH*H*-NH), 2.33 (t, J = 12.5 Hz, 1H, NH−C*H*H−C), 1.97 (d, J = 11.9 Hz, 1H, NH−CH*H*-C), 1.14 (s, 3H, C(CH_3)$_2$), 0.96 (s, 3H, C(CH_3)$_2$). ^{13}C NMR (101 MHz, d_8-THF, 298 k) δ 159.4 (*i*-Ph), 158.0 (*i*-Ph), 152.5 (*o*-Ph), 152.0 (*o*-Ph), 130.9 (*o*-Ph), 126.7 (*m*-Ph), 123.9 (*m*-Ph), 122.7 (*m*-Ph), 122.4 (*o*-Ph), 116.9 (*p*-Ph), 112.9 (*m*-Ph), 111.8 (*p*-Ph), 62.9 (OCH$_3$), 60.2 (Ph−CH_2−NH), 56.3 (Ph-CH_2−NH), 56.0 (Ph-CH_2−NH), 55.9 (O−CH_3), 54.5 (NH-CH_2−C), 33.6 (*C*(CH_3)$_2$), 26.9 (C(CH_3)$_2$), 26.7 (C(CH_3)$_2$). Elemental Analysis for $C_{21}H_{28}N_2O_4Zn$ (875 g/mol): Calculated: C, 57.61; H, 6.45; N, 6.40%. Found: C, 57.38; H, 6.31; N, 6.34%.

Synthesis of $\mathbf{L_{2b}Zn_2(OAc)_2}$ Mixture (from $\mathbf{L_{2b}H}$). To a solution of $\mathbf{L_{2b}H}$ (200 mg, 0.53 mmol) in MeOH (10 mL), a methanol solution of $Zn(OAc)_2{\cdot}2(H_2O)$ (235 mg, 1.07 mmol in 10 mL) was added. The reaction mixture was stirred at 22 °C for 16 h, prior to removal of all solvent, under reduced pressure. The resultant white powder was washed with pentane and dried under reduced pressure (yield: 71%, 235 mg). From dimer $\mathbf{(L_{2b})_2Zn_2}$: Under a nitrogen atmosphere, the dimer $\mathbf{(L_{2b})_2Zn_2}$ (100 mg, 0.23 mmol) was suspended in dry THF (3 mL). Subsequently, a suspension of $Zn(OAc)_2$ (41.9 mg, 0.23 mmol) in dry THF (2 mL) was added in one portion to the ligand solution. After the mixture stirred for 16 h at ambient temperature, all volatiles were removed under vacuum, and the product mixture was isolated as a white powder (yield: 64%, 92 mg). Elemental Analysis for $C_{25}H_{34}N_2O_8Zn_2$ (621 g/mol): Calculated: C, 48.33; H, 5.52; N, 4.51%. Found: C, 48.18; H, 5.63; N, 4.34%.

Synthesis of $\mathbf{(L_{2b})_2Zn_3(OAc)_4}$. A THF solution of $Zn(OAc)_2$ (88 mg, 0.4 mmol in 3 mL) was injected into a solution of $\mathbf{L_{2b}H}$ (100 mg, 0.27 mmol) in THF solvent (3 mL). The reaction mixture was stirred for 16 h at 22 °C, and then all solvent was removed in vacuo. The resultant white solid was washed with pentane and was dried under reduced pressure (yield: 85%, 244 mg). Elemental Analysis for $C_{46}H_{62}N_4O_{12}Zn_3$ (621 g/mol): Calculated: C, 52.16; H, 5.90; N, 5.29%. Found: C, 52.08; H, 5.59; N, 5.19%.

Synthesis of $\mathbf{L_{2b}Zn_3(OAc)_4}$. $\mathbf{L_{2b}H}$ (400 mg, 1.06 mmol) was dissolved in 20 mL of THF, and $Zn(OAc)_2$ (391 mg, 2.14 mmol) was subsequently added as a solid. After the mixture stirred for 16 h at ambient temperature, all solvent was removed under reduced pressure

DOI: 10.1021/acs.inorgchem.5b02233
Inorg. Chem. XXXX, XXX, XXX−XXX

to give $\mathbf{L_{2b}Zn_3(OAc)_4}$ as a white powder. The pure product was obtained by washing with pentane.

^{1}H NMR (400 MHz, C_6D_6, 298 K) δ 6.66 (m, 6H, Ph), 4.68 (br s, 2H, Ph−C*H*H-NH), 3.67 (s, 6H, O−CH_3), 2.98 (d, J = 11.6 Hz, 2H, Ph−CH*H*-NH), 2.82 (t, J = 12.7, 2H, NH−C*H*H-C), 1.93 (m, 6H, NH−CH*H*-C, and OAc), 1.82 (br t, J = 14.0 Hz, 3H, NH, and OAc), 0.45 (d, J = 6.4 Hz, 6H, C(CH_3)$_2$). ^{13}C NMR (101 MHz, C_6D_6, 298 K) δ 150.3 (*i*-Ph), 150.0 (*o*-Ph), 126.0 (*o*-Ph), 123.2 (*m*-Ph), 118.1 (*p*-Ph), 111.8 (*m*-Ph), 61.4 (NH-CH_2−C), 55.9 (O−CH_3), 54.0 (Ph-CH_2−NH), 33.7 (C(CH_3)$_2$), 27.9 (C(CH_3CH_3)), 22.4 (OAc), 20.0 (C(CH_3CH_3)). Elemental Analysis for $C_{29}H_{40}N_2O_{12}Zn_3$ (621 g/mol): Calculated: C, 48.33; H, 5.52; N, 4.51%; Found: C, 48.17; H, 5.63; N, 4.37%.

Synthesis of $\mathbf{L_{2b}Zn_2Et_2}$. Under a nitrogen atmosphere, $\mathbf{(L_{2b})_2Zn_2}$ (200 mg, 0.46 mmol) was suspended in dry THF (7 mL). A solution of $ZnEt_2$ (56 mg, 0.456 mmol) in dry THF (3 mL) was added dropwise into the previous solution to obtain a colorless solution. The reaction mixture was stirred at ambient temperature for 16 h, and then all volatiles were removed under reduced pressure to give $\mathbf{L_{2b}Zn_2Et_2}$ as a white powder (yield: 75%, 190 mg).

^{1}H NMR (400 MHz, C_6D_6, 298 K) δ 6.74 (dd, J = 7.1, 2.1 Hz, 2H, *m*-Ph), 6.65 (m, 4H, *m*-Ph + *p*-Ph), 4.29 (t, J = 11.7 Hz, 2H, Ph−C*H*H-NH), 3.52 (s, 6H, O−CH_3), 2.77 (d, J = 11.2 Hz, 2H, Ph−CH*H*-NH), 2.60 (t, J = 13.8, 11.3 Hz, 2H, NH−C*H*H-C), 2.05 (t, J = 8.1 Hz, 3H, Zn-CH_2CH_3), 1.79 (t, J = 8.1 Hz, 3H, Zn-CH_2CH_3), 1.69 (d, J = 11.50 Hz, 2H, NH−CH*H*-C), 0.94 (q, J = 8.1 Hz, 2H, Zn−CH_2CH_3), 0.86 (t, J = 13.3 Hz, 2H, N*H*), 0.61 (q, J = 8.1 Hz, 2H, Zn−CH_2CH_3), 0.35 (s, 3H, C(CH_3)$_2$), −0.37 (s, 3H, C(CH_3)$_2$). ^{13}C NMR (101 MHz, C_6D_6) δ 154.10 (*i*-Ph), 149.3 (*o*-Ph), 124.9 (*o*-Ph), 123.1 (*m*-Ph), 113.9 (*m*-Ph), 111.1 (*p*-Ph), 61.7 (NH−CH_2−C), 55.9 (O−CH_3), 54.8 (Ph−CH_2−NH), 33.6 (C(CH_3)$_2$), 27.8 (C(CH_3) (CH_3)), 20.5 (C(CH_3)(CH_3)), 15.0 (Zn-CH_2CH_3), 13.6 (Zn-CH_2CH_3), −1.7 (Zn-CH_2CH_3), −3.8 (Zn-CH_2CH_3). Elemental Analysis for $C_{25}H_{38}N_2O_4Zn_2$ (561 g/mol): Calculated: C, 53.49; H, 6.82; N, 4.99%. Found: C, 53.35; H, 7.19; N, 4.84%.

CO_2/CHO Polymerization Reactions at 1 bar of CO_2 Pressure. The zinc catalyst (1 equiv) was suspended in CHO (1 mL, 100 equiv) under nitrogen atmosphere in a Schlenk tube charged with a stirrer bar. The Schlenk tube was then connected to a CO_2 line, where the reaction mixture was degassed three times and then heated to 80 °C under 1 bar of CO_2 pressure. The crude polymer was obtained by evaporation of the remaining CHO under reduced pressure. Polymers were dissolved in THF and then purified by precipitation from MeOH to yield a white powder.

CO_2/CHO Polymerization Reactions at 30 bar of CO_2 Pressure. The zinc catalyst (1 equiv) was suspended in CHO (6 mL, 1000 equiv) under a nitrogen atmosphere in a Schlenk tube charged with a stirrer bar. The Paar reactor was purged five times with CO_2. The reaction mixture was then transferred into the reactor at 1 atm of CO_2 pressure. The pressure was then adjusted to 30 bar at 80 °C, unless otherwise stated. The crude polymer was obtained by evaporation of the remaining CHO under reduced pressure. Polymers were purified by precipitation from a THF solution in MeOH to yield a white powder.

PA/CHO Polymerization Reactions. The zinc catalyst (1 equiv) was suspended in CHO (1 mL, 800 equiv) under nitrogen atmosphere in screw cap vial charged with a stirrer bar. PA (100 equiv) was added, and the vial was closed, sealed, and heated to 100 °C. The crude polymer was obtained by evaporation of the remaining CHO under reduced pressure. Polymers were dissolved in THF then purified by precipitation from MeOH to yield a white powder.

Terpolymerization of PA/CO_2/CHO. $\mathbf{L_{2a}Zn_2(OAc)_2}$ (36.6 mg, 0.059 mmol, 1 equiv) and PA (877 mg, 5.93 mmol, 100 equiv) were suspended in CHO (6 mL, 59.3 mmol, 1000 equiv) under nitrogen atmosphere in Schlenk tube charged with a stirrer bar. The Parr reactor was purged five times with CO_2. The reaction mixture was then transferred into the reactor at 1 atm of CO_2 pressure. The pressure was then adjusted to 30 bar at 100 °C. Aliquots were taken after 2 and 18 h by a depressurization−repressurization procedure at 100 °C. The crude polymer was obtained by evaporation of the remaining CHO under reduced pressure. Polymers were purified by precipitation from a THF solution in MeOH to yield a white powder.

■ ASSOCIATED CONTENT

Ⓢ Supporting Information

The Supporting Information is available free of charge on the ACS Publications website at DOI: 10.1021/acs.inorgchem.5b02233.

The complete experimental procedures and characterization data for all new compounds and copolymers. (PDF)

Single-crystal X-ray structure information in CIF format. (CIF)

■ AUTHOR INFORMATION

Corresponding Author

*E-mail: c.k.williams@imperial.ac.uk.

Notes

The authors declare no competing financial interest.

■ ACKNOWLEDGMENTS

The EPSRC (EP/K035274/1; EP/K014070/1; EP/K014668; EP/L017393/1), Chemistry Innovation (Project No. 101688), and Climate KIC (studentship to A.T.) are acknowledged for research funding.

■ REFERENCES

(1) Zhang, W.; Loebach, J. L.; Wilson, S. R.; Jacobsen, E. N. *J. Am. Chem. Soc.* **1990**, *112* (7), 2801−2803.

(2) Irie, R.; Noda, K.; Ito, Y.; Matsumoto, N.; Katsuki, T. *Tetrahedron Lett.* **1990**, *31* (50), 7345−7348.

(3) (a) Gupta, K. C.; Sutar, A. K. *Coord. Chem. Rev.* **2008**, *252* (12−14), 1420−1450. (b) Venkataramanan, N. S.; Kuppuraj, G.; Rajagopal, S. *Coord. Chem. Rev.* **2005**, *249* (11−12), 1249−1268.

(4) (a) Liu, Y.; Ren, W.-M.; He, K.-K.; Lu, X.-B. *Nat. Commun.* **2014**, *5*. (b) Wang, X.; Thevenon, A.; Brosmer, J. L.; Yu, I.; Khan, S. I.; Mehrkhodavandi, P.; Diaconescu, P. L. *J. Am. Chem. Soc.* **2014**, *136* (32), 11264−11267. (c) Bakewell, C.; White, A. J. P.; Long, N. J.; Williams, C. K. *Angew. Chem., Int. Ed.* **2014**, *53* (35), 9226−9230. (d) Childers, M. I.; Longo, J. M.; Van Zee, N. J.; LaPointe, A. M.; Coates, G. W. *Chem. Rev.* **2014**, *114* (16), 8129−8152. (e) Bakewell, C.; Cao, T.-P.-A.; Long, N.; Le Goff, X. F.; Auffrant, A.; Williams, C. K. *J. Am. Chem. Soc.* **2012**, *134* (51), 20577−20580. (f) Dijkstra, P. J.; Du, H.; Feijen, J. *Polym. Chem.* **2011**, *2* (3), 520−527. (g) Darensbourg, D. J. *Chem. Rev.* **2007**, *107* (6), 2388−2410. (h) Hormnirun, P.; Marshall, E. L.; Gibson, V. C.; Pugh, R. I.; White, A. J. P. *Proc. Natl. Acad. Sci. U. S. A.* **2006**, *103* (42), 15343−15348. (i) Cohen, C. T.; Chu, T.; Coates, G. W. *J. Am. Chem. Soc.* **2005**, *127* (31), 10869−10878. (j) Qin, Z.; Thomas, C. M.; Lee, S.; Coates, G. W. *Angew. Chem., Int. Ed.* **2003**, *42* (44), 5484−5487. (k) Zhong, Z.; Dijkstra, P. J.; Feijen, J. *J. Am. Chem. Soc.* **2003**, *125* (37), 11291−11298. (l) Ovitt, T. M.; Coates, G. W. *J. Am. Chem. Soc.* **2002**, *124* (7), 1316−1326. (m) Jhurry, D.; Bhaw-Luximon, A.; Spassky, N. *Macromol. Symp.* **2001**, *175* (1), 67−80.

(5) (a) Baleizão, C.; Garcia, H. *Chem. Rev.* **2006**, *106* (9), 3987−4043. (b) McGarrigle, E. M.; Gilheany, D. G. *Chem. Rev.* **2005**, *105* (5), 1563−1602.

(6) (a) Mechler, M.; Latendorf, K.; Frey, W.; Peters, R. *Organometallics* **2013**, *32* (1), 112−130. (b) Golchoubian, H.; Mardani, H. R.; Bruno, G.; Rudbari, H. A. *Polyhedron* **2012**, *44* (1), 44−51. (c) Thurston, J. H.; Tang, C. G. Z.; Trahan, D. W.; Whitmire, K. H. *Inorg. Chem.* **2004**, *43* (8), 2708−2713. (d) Liable-Sands, L. M.; Incarvito, C.; Rheingold, A. L.; Qin, C. J.; Gavrilova, A. L.; Bosnich, B. *Inorg. Chem.* **2001**, *40* (9), 2147−2155.

DOI: 10.1021/acs.inorgchem.5b02233
Inorg. Chem. XXXX, XXX, XXX−XXX

(7) (a) Xie, Q.-W.; Wu, S.-Q.; Liu, C.-M.; Cui, A.-L.; Kou, H.-Z. *Dalton Trans.* **2013**, *42* (31), 11227−11233. (b) Binnemans, K.; Lodewyckx, K.; Donnio, B.; Guillon, D. *Chem. - Eur. J.* **2002**, *8* (5), 1101−1105. (c) Kahn, M. L.; Rajendiran, T. M.; Jeannin, Y.; Mathonière, C.; Kahn, O. *C. R. Acad. Sci., Ser. IIc: Chim.* **2000**, *3* (2), 131−137. (d) Ramade, I.; Kahn, O.; Jeannin, Y.; Robert, F. *Inorg. Chem.* **1997**, *36* (5), 930−936.

(8) Xie, Q.-W.; Wu, S.-Q.; Shi, W.-B.; Liu, C.-M.; Cui, A.-L.; Kou, H.-Z. *Dalton Trans.* **2014**, *43* (29), 11309−11316.

(9) Matsunaga, S.; Shibasaki, M. *Chem. Commun.* **2014**, *50* (9), 1044−1057.

(10) (a) Buchard, A.; Jutz, F.; Kember, M. R.; White, A. J. P.; Rzepa, H. S.; Williams, C. K. *Macromolecules* **2012**, *45* (17), 6781−6795. (b) Klaus, S.; Lehenmeier, M. W.; Herdtweck, E.; Deglmann, P.; Ott, A. K.; Rieger, B. *J. Am. Chem. Soc.* **2011**, *133* (33), 13151−13161. (c) Jutz, F.; Buchard, A.; Kember, M. R.; Fredriksen, S. B.; Williams, C. K. *J. Am. Chem. Soc.* **2011**, *133* (43), 17395−17405. (d) Cheng, M.; Moore, D. R.; Reczek, J. J.; Chamberlain, B. M.; Lobkovsky, E. B.; Coates, G. W. *J. Am. Chem. Soc.* **2001**, *123* (36), 8738−8749.

(11) (a) Saini, P. K.; Romain, C.; Williams, C. K. *Chem. Commun.* **2014**, *50* (32), 4164−4167. (b) Kember, M. R.; Williams, C. K. *J. Am. Chem. Soc.* **2012**, *134* (38), 15676−15679. (c) Kember, M. R.; Jutz, F.; Buchard, A.; White, A. J. P.; Williams, C. K. *Chem. Sci.* **2012**, *3* (4), 1245−1255. (d) Buchard, A.; Kember, M. R.; Sandeman, K. G.; Williams, C. K. *Chem. Commun.* **2011**, *47* (1), 212−214. (e) Kember, M. R.; White, A. J. P.; Williams, C. K. *Macromolecules* **2010**, *43* (5), 2291−2298. (f) Kember, M. R.; White, A. J. P.; Williams, C. K. *Inorg. Chem.* **2009**, *48* (19), 9535−9542. (g) Kember, M. R.; Knight, P. D.; Reung, P. T. R.; Williams, C. K. *Angew. Chem., Int. Ed.* **2009**, *48* (5), 931−933.

(12) (a) Ellis, W. C.; Jung, Y.; Mulzer, M.; Di Girolamo, R.; Lobkovsky, E. B.; Coates, G. W. *Chem. Sci.* **2014**, *5* (10), 4004−4011. (b) Moore, D. R.; Cheng, M.; Lobkovsky, E. B.; Coates, G. W. *J. Am. Chem. Soc.* **2003**, *125* (39), 11911−11924. (c) Allen, S. D.; Moore, D. R.; Lobkovsky, E. B.; Coates, G. W. *J. Am. Chem. Soc.* **2002**, *124* (48), 14284−14285. (d) Moore, D. R.; Cheng, M.; Lobkovsky, E. B.; Coates, G. W. *Angew. Chem., Int. Ed.* **2002**, *41* (14), 2599−2602.

(13) (a) Xiao, Y.; Wang, Z.; Ding, K. *Macromolecules* **2006**, *39* (1), 128−137. (b) Xiao, Y.; Wang, Z.; Ding, K. *Chem. - Eur. J.* **2005**, *11* (12), 3668−3678.

(14) (a) Chatterjee, C.; Chisholm, M. H.; El-Khaldy, A.; McIntosh, R. D.; Miller, J. T.; Wu, T. *Inorg. Chem.* **2013**, *52* (8), 4547−4553. (b) Harrold, N. D.; Li, Y.; Chisholm, M. H. *Macromolecules* **2013**, *46* (3), 692−698. (c) Chatterjee, C.; Chisholm, M. H. *Inorg. Chem.* **2012**, *51* (21), 12041−12052. (d) Chatterjee, C.; Chisholm, M. H. *Inorg. Chem.* **2011**, *50* (10), 4481−4492. (e) Sugimoto, H.; Ohshima, H.; Inoue, S. *J. Polym. Sci., Part A: Polym. Chem.* **2003**, *41* (22), 3549−3555. (f) Mang, S.; Cooper, A. I.; Colclough, M. E.; Chauhan, N.; Holmes, A. B. *Macromolecules* **2000**, *33* (2), 303−308. (g) Takeda, N.; Inoue, S. *Makromol. Chem.* **1978**, *179* (5), 1377−1381.

(15) (a) Bok, T.; Yun, H.; Lee, B. Y. *Inorg. Chem.* **2006**, *45* (10), 4228−4237. (b) Lee, B. Y.; Kwon, H. Y.; Lee, S. Y.; Na, S. J.; Han, S.-i.; Yun, H.; Lee, H.; Park, Y.-W. *J. Am. Chem. Soc.* **2005**, *127* (9), 3031−3037.

(16) (a) Paul, S.; Zhu, Y.; Romain, C.; Brooks, R.; Saini, P. K.; Williams, C. K. *Chem. Commun.* **2015**, *51* (30), 6459−6479. (b) Romain, C.; Thevenon, A.; Saini, P.; Williams, C. *Dinuclear Metal Complex-Mediated Formation of CO2-Based Polycarbonates*. Springer: Berlin Heidelberg, 2015; pp 1−41.

(17) Lehenmeier, M. W.; Kissling, S.; Altenbuchner, P. T.; Bruckmeier, C.; Deglmann, P.; Brym, A.-K.; Rieger, B. *Angew. Chem., Int. Ed.* **2013**, *52* (37), 9821−9826.

(18) Kissling, S.; Lehenmeier, M. W.; Altenbuchner, P. T.; Kronast, A.; Reiter, M.; Deglmann, P.; Seemann, U. B.; Rieger, B. *Chem. Commun.* **2015**, *51* (22), 4579−4582.

(19) Kissling, S.; Altenbuchner, P. T.; Lehenmeier, M. W.; Herdtweck, E.; Deglmann, P.; Seemann, U. B.; Rieger, B. *Chem. - Eur. J.* **2015**, *21* (22), 8148−8157.

(20) (a) Lu, X.-B.; Darensbourg, D. J. *Chem. Soc. Rev.* **2012**, *41* (4), 1462−1484. (b) Lu, X.-B.; Wang, Y. *Angew. Chem., Int. Ed.* **2004**, *43* (27), 3574−3577. (c) Darensbourg, D. J.; Mackiewicz, R. M.; Phelps, A. L.; Billodeaux, D. R. *Acc. Chem. Res.* **2004**, *37* (11), 836−844. (d) Eberhardt, R.; Allmendinger, M.; Rieger, B. *Macromol. Rapid Commun.* **2003**, *24* (2), 194−196. (e) Darensbourg, D. J.; Yarbrough, J. C. *J. Am. Chem. Soc.* **2002**, *124* (22), 6335−6342.

(21) Nakano, K.; Kamada, T.; Nozaki, K. *Angew. Chem., Int. Ed.* **2006**, *45* (43), 7274−7277.

(22) (a) Darensbourg, D. J.; Chung, W.-C.; Wilson, S. J. *ACS Catal.* **2013**, *3* (12), 3050−3057. (b) Li, H.; Niu, Y. *Polym. J.* **2011**, *43* (2), 121−125.

(23) (a) Cyriac, A.; Jeon, J. Y.; Varghese, J. K.; Park, J. H.; Choi, S. Y.; Chung, Y. K.; Lee, B. Y. *Dalton Trans.* **2012**, *41* (5), 1444−1447. (b) Ren, W.-M.; Liu, Y.; Wu, G.-P.; Liu, J.; Lu, X.-B. *J. Polym. Sci., Part A: Polym. Chem.* **2011**, *49* (22), 4894−4901. (c) Yoo, J.; Na, S. J.; Park, H. C.; Cyriac, A.; Lee, B. Y. *Dalton Trans.* **2010**, *39* (10), 2622−2630. (d) Ren, W.-M.; Zhang, X.; Liu, Y.; Li, J.-F.; Wang, H.; Lu, X.-B. *Macromolecules* **2010**, *43* (3), 1396−1402. (e) Na, S. J.; S, S.; Cyriac, A.; Kim, B. E.; Yoo, J.; Kang, Y. K.; Han, S. J.; Lee, C.; Lee, B. Y. *Inorg. Chem.* **2009**, *48* (21), 10455−10465. (f) Ren, W.-M.; Liu, Z.-W.; Wen, Y.-Q.; Zhang, R.; Lu, X.-B. *J. Am. Chem. Soc.* **2009**, *131* (32), 11509−11518. (g) S, S.; Min, J. K.; Seong, J. E.; Na, S. J.; Lee, B. Y. *Angew. Chem., Int. Ed.* **2008**, *47* (38), 7306−7309. (h) Noh, E. K.; Na, S. J.; S, S.; Kim, S.-W.; Lee, B. Y. *J. Am. Chem. Soc.* **2007**, *129* (26), 8082−8083.

(24) Nakano, K.; Hashimoto, S.; Nozaki, K. *Chem. Sci.* **2010**, *1* (3), 369−373.

(25) (a) Liu, Y.; Ren, W.-M.; Liu, J.; Lu, X.-B. *Angew. Chem., Int. Ed.* **2013**, *52* (44), 11594−11598. (b) Vagin, S. I.; Reichardt, R.; Klaus, S.; Rieger, B. *J. Am. Chem. Soc.* **2010**, *132* (41), 14367−14369. (c) Thomas, R. M.; Widger, P. C. B.; Ahmed, S. M.; Jeske, R. C.; Hirahata, W.; Lobkovsky, E. B.; Coates, G. W. *J. Am. Chem. Soc.* **2010**, *132* (46), 16520−16525. (d) Hirahata, W.; Thomas, R. M.; Lobkovsky, E. B.; Coates, G. W. *J. Am. Chem. Soc.* **2008**, *130* (52), 17658−17659. (e) Ready, J. M.; Jacobsen, E. N. *Angew. Chem., Int. Ed.* **2002**, *41* (8), 1374−1377.

(26) Li, C.-H.; Chuang, H.-J.; Li, C.-Y.; Ko, B.-T.; Lin, C.-H. *Polym. Chem.* **2014**, *5* (17), 4875−4878.

(27) Bakewell, C.; Fateh-Iravani, G.; Beh, D. W.; Myers, D.; Tabthong, S.; Hormnirun, P.; White, A. J. P.; Long, N.; Williams, C. K. *Dalton Trans.* **2015**, *44* (27), 12326−12337.

(28) (a) Andruh, M. *Dalton Trans.* **2015**, *44*, 16633. (b) Lü, X.-Q.; Feng, W.-X.; Hui, Y.-N.; Wei, T.; Song, J.-R.; Zhao, S.-S.; Wong, W.-Y.; Wong, W.-K.; Jones, R. A. *Eur. J. Inorg. Chem.* **2010**, *2010* (18), 2714−2722. (c) Mihara, H.; Xu, Y.; Shepherd, N. E.; Matsunaga, S.; Shibasaki, M. *J. Am. Chem. Soc.* **2009**, *131* (24), 8384−8385. (d) Bi, W.-Y.; Lü, X.-Q.; Chai, W.-L.; Song, J.-R.; Wong, W.-Y.; Wong, W.-K.; Jones, R. A. *J. Mol. Struct.* **2008**, *891* (1−3), 450−455.

(29) Addison, A. W.; Rao, T. N.; Reedijk, J.; van Rijn, J.; Verschoor, G. C. *J. Chem. Soc., Dalton Trans.* **1984**, *7*, 1349−1356.

(30) Wu, L.-y.; Fan, D.-d.; Lu, X.-q.; Lu, R. *Chin. J. Polym. Sci.* **2014**, *32* (6), 768−777.

(31) Armstrong, D. R.; Garden, J. A.; Kennedy, A. R.; Leenhouts, S. M.; Mulvey, R. E.; O'Keefe, P.; O'Hara, C. T.; Steven, A. *Chem. - Eur. J.* **2013**, *19* (40), 13492−13503.

(32) Shakya, R.; Wang, Z.; Powell, D. R.; Houser, R. P. *Inorg. Chem.* **2011**, *50* (22), 11581−11591.

(33) (a) Saini, P. K.; Romain, C.; Zhu, Y.; Williams, C. K. *Polym. Chem.* **2014**, *5* (20), 6068−6075. (b) Huijser, S.; Hosseini Nejad, E.; Sablong, R.; Jong, C. d.; Koning, C. E.; Duchateau, R. *Macromolecules* **2011**, *44* (5), 1132−1139.

(34) Ishida, T.; Watanabe, R.; Fujiwara, K.; Okazawa, A.; Kojima, N.; Tanaka, G.; Yoshii, S.; Nojiri, H. *Dalton Trans.* **2012**, *41* (44), 13609−13619.

DOI: 10.1021/acs.inorgchem.5b02233
Inorg. Chem. XXXX, XXX, XXX−XXX